

EFSUMB Course Book, 2nd Edition

Editor: Christoph F. Dietrich

Ultrasound of the urinary bladder

¹Felix Trinkler, ²Christoph F Dietrich

¹UroZentrum Zürich, UroZentrum Zollikon AG, Forchstrasse 424, 8702 Zollikon, Switzerland.

²Medizinische Klinik 2, Caritas-Krankenhaus Bad Mergentheim, Uhlandstr. 7, 97980 Bad Mergentheim, Germany.

Corresponding author:

Prof. Dr. Christoph F. Dietrich, MBA

Medizinische Klinik 2, Caritas-Krankenhaus Bad Mergentheim, Uhlandstr. 7, 97980 Bad Mergentheim, Germany

Tel.: (+) 49 - 7931 – 58 – 2201

Fax: (+) 49 - 7931 – 58 – 2290

Email: christoph.dietrich@ckbm.de

Acknowledgments: None.

Topographical remarks

The urinary bladder is part of the lower urinary tract and is located intra-abdominally sheltered within the bony pelvis. Traumatic bladder lesions are found mostly in polytrauma patients with associated pelvic fractures. The bladder is anchored to the anterior abdominal wall by the obliterated urachus. The bladder neck is fixed by the pelvic fascia. Against the pelvic side walls, it is cushioned by perivesical fat within the retropubic Retzius' space. The pelvic floor muscles, located caudally to the bladder, are important for urinary continence, especially in females. Only a part of the bladder is located retroperitoneally. The bladder dome sits next to the abdominal cavity; this is an important fact for the clinician to be aware of in order to avoid iatrogenic perforation during transurethral resection of the urinary bladder (TUR-B) or by insertion of suprapubic cystostomy tubes. In males, the bladder base is next to the prostate, the seminal vesicles, the ampullae of vas deferens and the rectum. In females, the posterior bladder wall is next to the vagina, the uterus and the adnexa.

Bladder anatomy

Anatomical considerations

The function of the bladder is urine storage and micturition. A normal bladder capacity is approximately 500 ml. The bladder is composed of contractile smooth muscle layers (detrusor vesicae muscle), an outer adventitia and lined by an inner mucosal layer (urothelium). The triangle between the two ureteric orifices and the urethral meatus at the bladder neck is called the trigone of the bladder. The vesical blood supply runs within the lateral and posterior bladder pedicles.

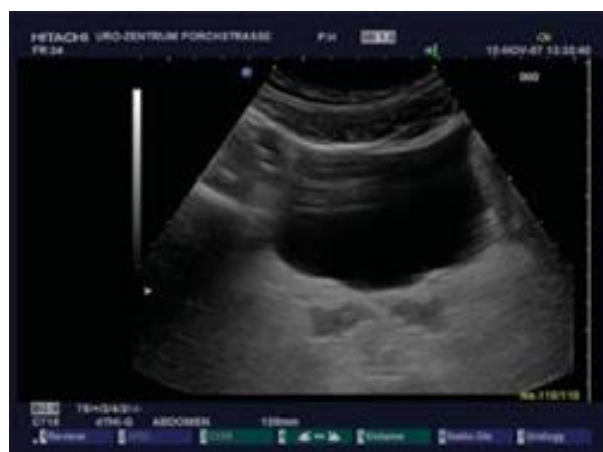
Echogenicity of the bladder and bladder content

When filled with urine the bladder content should be anechoic. Within the anechoic urine reverberation artefacts can often be seen [Figures 1 and 2].

Figure 1 Suprapubic abdominal ultrasound examination of the bladder. The bladder of this young male is partially filled with 257 ml of clear urine. Healthy bladder content should appear anechoic.



Figure 2 Suprapubic transverse scan of the bladder in a young male. Dorsal to the bladder, the symmetrical seminal vesicles can be seen. Behind the bladder roof hyperechoic reverberation echoes are often seen. This ultrasound artefact is produced by multiple reflections of an object if the acoustic impedances are too different (body to water). In this case the sound waves are reflected back into the bladder from the transducer-skin interface.



On ultrasound the bladder wall appears as a three layer structure. The detrusor muscle is of medium homogeneous echogenicity. The outer serosa (adventitia) layer and the inner

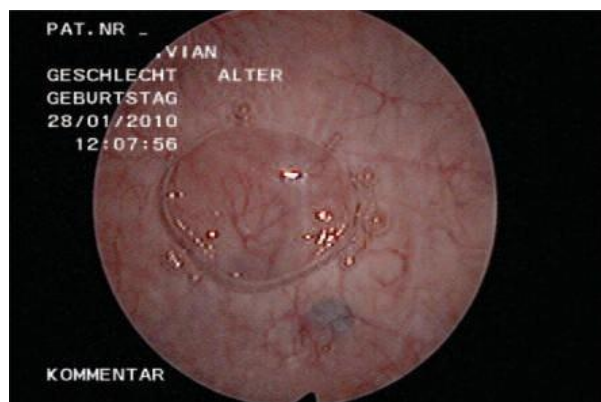
mucosa (urothelial) layer are hyperechoic compared with the middle detrusor smooth muscle (muscularis propria) layer [Figure 3].

Figure 3 The normal bladder wall is 3–5 mm thick. The thickness of the bladder wall depends on how full it is. In a full bladder, the thickness decreases to approximately 2–3 mm.



When filled, a normal bladder wall should have a uniform appearance without any contour irregularity [Figure 4].

Figure 4 Healthy bladders have a plain appearance when filled. This image shows the cystoscopic aspect of the female bladder. We can see air bubbles on the roof and a normal looking mucosa.



Examination technique

Transducers and patient position

The easiest way to scan the urinary bladder is by an external suprapubic abdominal approach with a convex 2.5–5 MHz probe. Most general ultrasound practitioners will have this type of abdominal probe as part of their standard equipment. The patient is examined in the supine position with a partially full bladder (200–300 ml). If it is necessary to obtain more detailed information of the bladder roof, linear probes with higher frequencies (7.5–16 MHz) can be used. The bladder floor and the distal and intramural part of the ureters can be visualised more accurately endosonographically in a lithotomy position with a higher frequency transrectal ultrasound (TRUS) in men, or with a vaginal probe in women [Figures 5 and 6]. In the same way as other organs, the bladder should be carefully scanned in transverse and longitudinal sections. A transurethral approach into the bladder with high-frequency mini probes for bladder cancer staging purposes is not yet a standard procedure.

Figure 5 Transrectal ultrasound of the bladder. Urine from the right ostium is seen just above the right seminal vesicle in a 34 year old male.

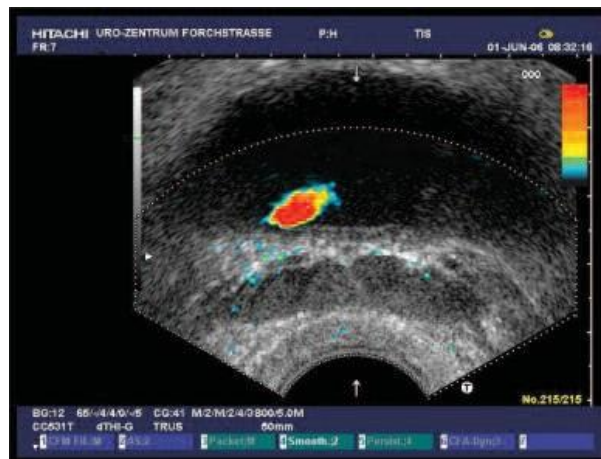


Figure 6 Endosonography with 360° high-frequency (20 MHz) mini probe with a 6-Fr diameter. Used for endourological staging of bladder cancer or urothelial cancer in the upper urinary tract, or in the detection of aberrant lower pole kidney vessels, which are responsible for ureteropelvic junction obstruction.



Diffuse bladder disease

Assessment of diffuse bladder disease should include sonographic evaluation of the bladder wall thickness, bladder shape and bladder content (echogenicity, capacity and post-void residual urine).

Detection and characterisation of diffuse bladder lesions

Bladder outlet obstruction

Bladder outlet obstruction (BOO) is the most common reason for diffuse morphological and physiological bladder changes. Subvesical obstruction has a very different aetiology. The most frequent cause in males is benign prostatic hyperplasia (BPH). BOO leads to lower urinary tract symptoms (LUTS), infections and bladder stones owing to residual post-void urine. The different inter-individual subjective estimations of the symptoms of LUTS can be documented with the International Prostate Symptom Score (IPSS). In BOO, the detrusor smooth muscle compensates for increasing subvesical resistance with detrusor hypertrophy, which results in

higher intravesical voiding pressure. The morphological expression of this compensatory upregulation against subvesical resistance is an increase in muscle mass (muscle hypertrophy) and collagen deposition, which results in detrusor trabeculations and pseudodiverticula formation. In this early stage (BPH stage 1) the high pressure results in clinically irritative voiding and symptoms ranging from frequency and urgency to urge incontinence (known as overactive bladder symptoms (OAB)) owing to low bladder compliance with small capacity because of collagen deposition and over-activity. The collagen accumulation in high pressure voiding bladders may be a result of poor blood supply and poor oxygenation as a result of high intramural tension. Depending on the severity of the subvesical obstruction, the detrusor smooth muscle may decompensate (BPH stage 2) by losing contractility, which results in a large capacity floppy bladder with high post-void residual urine volumes. Symptoms are nocturia, acute urinary retention or urinary overflow incontinence. Bladder compliance changes throughout the course of BOO are not yet fully understood; however, it is important to be aware that most of the symptoms of BOO, such as urgency, are caused by autonomous adaptation of the detrusor muscle to subvesical obstruction.

The following structures are assessed in sonographic evaluation of BOO:

- The bladder wall
- The bladder shape
- Bladder content.

The bladder wall

Detrusor hypertrophy results in the thickening of the bladder wall and in augmentation of the bladder wall mass (BWM). Bladder wall thickness (BWT) can be directly measured with ultrasound by measuring the anterior bladder wall transabdominally with a 7.5 MHz probe (or the posterior wall with a TRUS probe) with a defined bladder volume of 100–300 ml. Unobstructed normal BWT was found to be 3.0 ± 1.1 mm. A strong correlation between BOO and a BWT of greater than 5 mm at 150 ml filling was demonstrated [Figure 7]. The problem with BWT measurement is that the BWT is volume dependent. There is no standard bladder volume for BWT measurement in a non-invasive setting. The use of catheterisation for BWT

makes this an invasive diagnostic test. At present the bladder volume for BWT measurement is not standardised [Figures 7 and 8].

Using BWT and bladder volume, the BWM can be calculated by multiplying the bladder volume by the wall thickness and the specific gravity of bladder tissue ($0.957 \pm 0.026 \text{ g/cm}^3$). There is a cut-off weight for an obstructed bladder of $>50 \text{ g}$. BWM of more than 80 g suggests irreversible changes to the bladder detrusor muscle. However, the problem in BWM measurement is the interobserver and intraobserver variability and the fact that the bladder shape is never an absolute sphere in real life when using the bladder volume calculation. Uroflowmetry is an easy test to gain information about bladder voiding function, but it cannot discriminate between BOO and detrusor underactivity. Non-invasive BWT combined with BWM testing could provide the missing information about bladder contractility for the differential diagnosis between BOO and a 'floppy' underactive bladder, in cases of low flow. The gold standard for the accurate evaluation of bladder contractility and BOO is still the invasive and expensive urodynamic pressure-flow study.

Figure 7 Bladder wall thickness (BWT) 6.2–10.9 mm in a male with benign prostatic hyperplasia stage 2 with a post-void residual urine volume of 60 ml. BPH with a prostate volume of 70 cm^3 and median lobe hyperplasia. Transrectal ultrasound biopsy could exclude the suspicion of malignancy because of elevated prostate specific antigen $>4 \text{ ng/ml}$. BWT of more than 5 mm is suggestive of bladder outlet obstruction despite the measurement being taken after voiding and without the standardised bladder volume of 150 ml.



Figure 8 Bladder wall thickness measured on the anterior bladder wall with a linear probe (6.5 MHz) in a male with benign prostatic hyperplasia and bladder outlet obstruction.



The bladder shape

The bladder adaptation mechanism to compensate for chronic BOO is bladder muscle hyperplasia. The morphological changes are diffuse trabeculation of the detrusor muscle and formation of diffuse so called pseudodiverticula. A primary congenital diverticulum of the bladder is a malformation of the bladder muscle layer with an absent detrusor muscle and extravesimal protuberance of the mucosal layer [Figure 9]. They are often located behind the prostate on the bladder floor and are usually not associated with generalised bladder wall thickening. In contrast, pseudodiverticula are a diffuse secondary bladder reaction in BOO. Pseudodiverticula are secondary acquired pulsion diverticula and often have a narrow neck [Figures 9–11].

Figure 9 Typical cystoscopic appearance of trabeculation of the detrusor muscle in a patient with benign prostatic hyperplasia and bladder outlet obstruction. The hypertrophy of the detrusor muscle results in thickening of the bladder wall and formation of muscle trabeculation as a morphological sign of high pressure voiding.

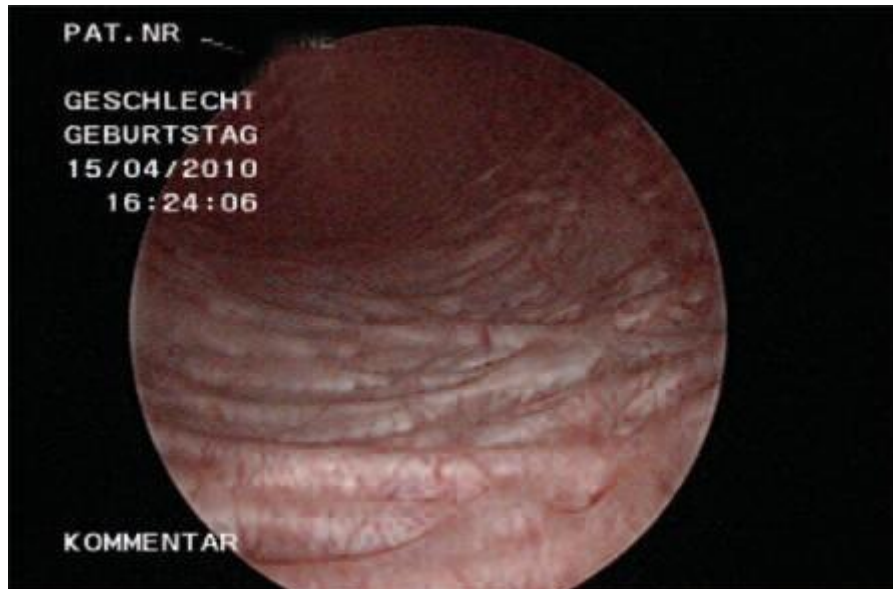


Figure 10 Typical sonographic appearance of trabeculation and diffuse formation of pseudodiverticula in a patient with benign prostatic hyperplasia and bladder outlet obstruction. During high pressure voiding of the bladder, the thinner mucosa and flattened muscle layer protrudes outwards between the hypertrophic trabecula.

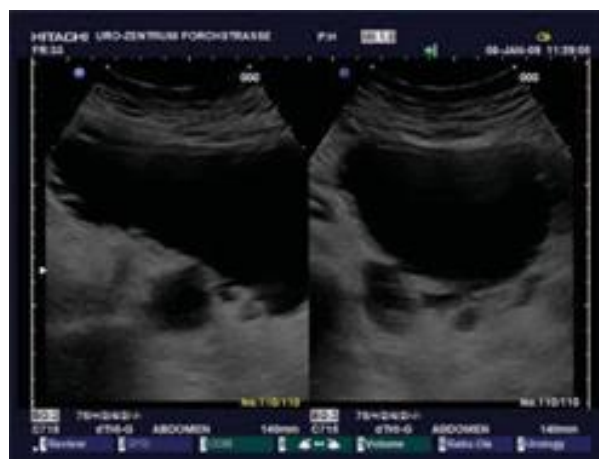
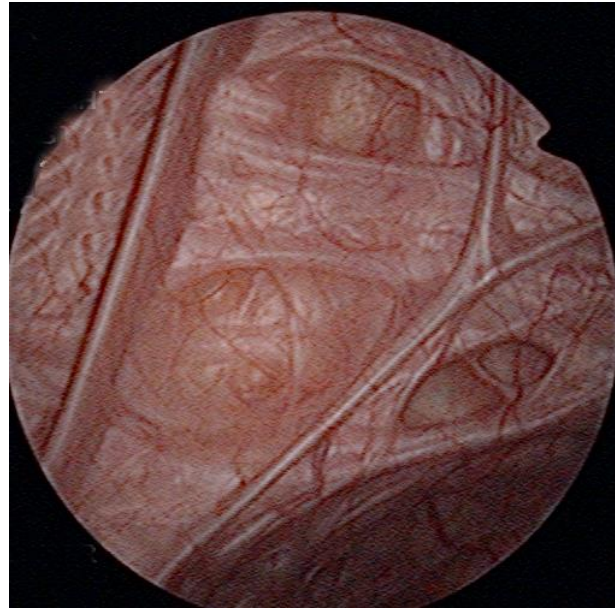


Figure 11 Cystoscopy showing diffuse formation of pseudodiverticula in a patient with benign prostatic hyperplasia and bladder outlet obstruction.



Bladder content

Bladder volume can be calculated by scanning the bladder transversely and longitudinally and using the following ellipsoid formula:

$$\text{Volume} = \text{height} \times \text{width} \times \text{depth} \times 0.5236$$

However, the bladder is never completely spherical, therefore volume calculations must allow for some measurement error [Figures 12–18]. Ultrasound bladder volume measurement is clinically important in defining the post-void residual urine in patients with bladder voiding disorders, especially BOO. As already mentioned, the BPH obstructive stage can be estimated non-invasively by IPSS, uroflowmetry and ultrasound post-void residual urine measurement. The differential diagnosis of overflow incontinence is easily confirmed with bladder ultrasound by detection of an overdistended bladder. Normal urine appears anechoic; in patients with chronic bladder infection the bladder content appears cloudy because of the reflection of leucocytes and proteins.

Figure 12 Measurement of post-void residual urine (153 ml) with the ellipsoid formula ($69.9 \times 61.2 \times 68.3 \text{ mm} \times 0.52 = 153 \text{ ml}$) in a 72 year old male with benign prostatic hyperplasia stage 2. Note the bladder wall is thickened with trabeculation.



Figure 13 Measurement of post-void residual urine in a young male. The normal bladder is empty after voiding (<1 ml).



Figure 14 Overflow incontinence with an over-distended bladder. The residual urine measured by ultrasound was 1049 ml; however, after catheterisation 1500 ml was drained. Therefore, it should be noted that in high bladder volumes ultrasound volume calculation underestimates volume.



Figure 15 Acute urinary retention in a 55 year old male with chronic prostatic obstruction and an over-distended detrusor muscle. A volume of 1800 ml clear urine was drained by catheterisation.

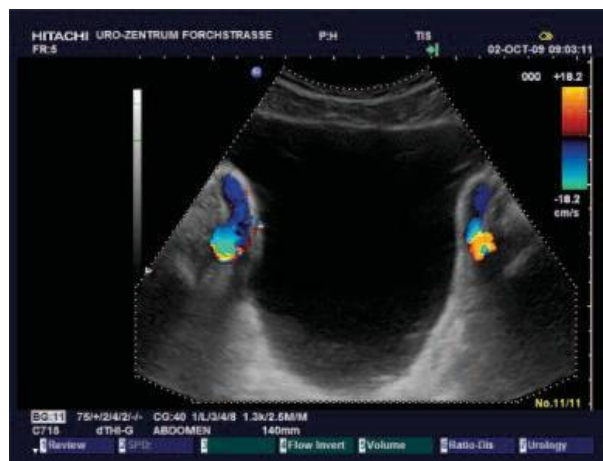


Figure 16 Chronic bacterial bladder infection in a female patient with a post-void residual volume of 139 ml. The urine appears cloudy as a result of chronic infection.



Figure 17 An 80 year old male with a permanent transurethral catheter for treatment of bladder outlet obstruction. The bladder content is cloudy because of chronic urinary tract infection.



Figure 18 Infected urine appears cloudy in a male with a continent ileal pouch who self-catheterises through a continent umbilical Mitrofanoff appendix valve. The patient has a history of a radical cystectomy after bladder cancer Stage pT3, G3 with pTis involvement of the prostate urethra.



Focal bladder disease

Detection and characterisation of focal bladder lesions

Approximately 95% of all focal bladder wall lesions represent transitional cell carcinomas (TCC). Most of these are found during examination of painless macroscopic haematuria or chronic microscopic haematuria. Large carcinomas are detected easily on ultrasound, however a full bladder is required for the examination because TCCs are hard to detect in empty bladders and small TCCs (<5 mm) in particular are rarely seen on ultrasound. Approximately 10% of TCCs diagnosed on ultrasound are false-positives owing to bladder wall trabeculation, a prominent interureteric crest, calculi, haematoma or focal cystitis. Colour Doppler ultrasound is not always helpful in the differentiation between clots and bladder tumours because colour Doppler signals in tumours are not often present as they are in haematomas. Contrast enhanced ultrasound (CEUS) is more accurate in these cases. Therefore, bladder ultrasound is not recommended for the exclusion of TCCs in haematuria. All sonographically suspicious focal bladder lesions should be examined with careful

cystoscopy. Even virtual cystoscopy with CT is inadequate in the detection of TCCs because flat tumours (carcinoma in situ, pTis) are not detected.

Focal bladder wall lesions

Bladder tumours (neoplasia)

Over 90% of all tumours of the bladder are TCCs. The incidence increases with age and they are usually found in patients between 65 and 70 years old. Tobacco smokers have a four-fold higher risk of developing a TCC. Rarer entities include squamous cell carcinoma (1%), adenocarcinoma (<2%) and urachal carcinoma (0.07–0.7%). TCC has a multifactorial origin. TCCs have a high recurrence rate at different times and different sites (multifocal). It is a systemic cancer with lymphatic spread; metastases form when TCC invades the bladder muscle layer (\geq cT2) [Figures 19-26] [(1-3)].

Figure 19 Sonographic appearance of a papillary transitional cell carcinoma in a male with obstructive benign prostatic hyperplasia and macrohaematuria. Note the non-anechoic urine as a result of haematuria as well as the thickened bladder wall.



Figure 20 Cystoscopic appearance of a papillary transitional cell carcinoma.

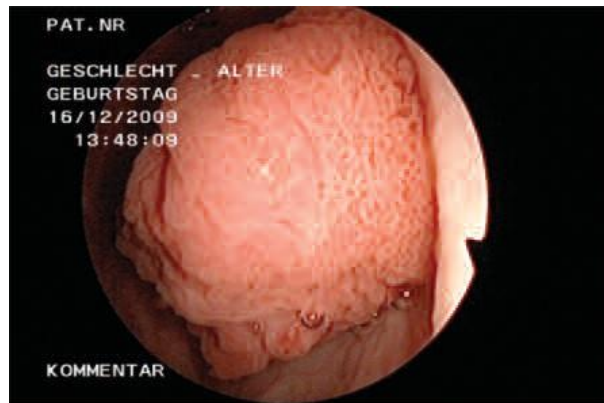


Figure 21 The pitfall of bladder ultrasound: small transitional cell carcinomas, such as pTa, G1 or pTis, G3 (flat tumour) cannot be detected with bladder ultrasound. Cystoscopy is mandatory in all suspicious focal bladder lesions.

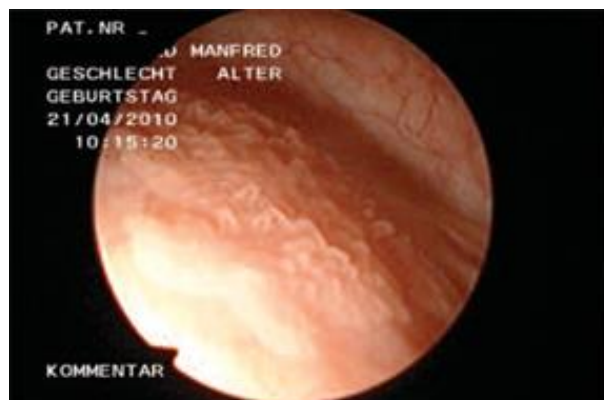


Figure 22 Solitary focal bladder wall lesion, which is sonographically highly suspicious of transitional cell carcinoma. However, cystoscopy revealed a clot adhering to the wall. This is a false-positive ultrasound diagnosis.

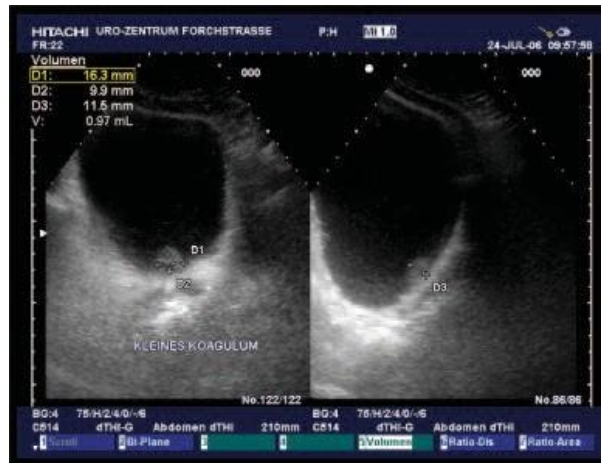


Figure 23 Small transitional cell carcinomas (TCC) are generally not easy to see on bladder ultrasound. In this case, a small TCC can be seen on the posterior bladder wall.



Figure 24 Colour Doppler bladder ultrasound. A small transitional cell carcinoma can be seen behind the right ostium. A ureteric urine jet is detectable, but no perfusion is seen within the tumour (same patient as shown in Figure 23).

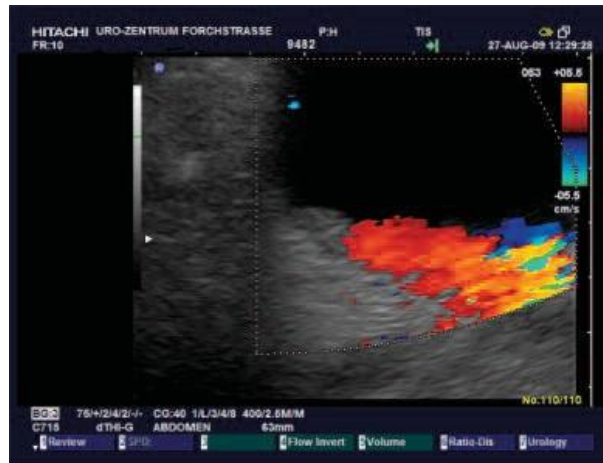


Figure 25 Colour Doppler in bladder ultrasound of a female patient. If perfusion within the tumour can be detected, then the diagnosis of this focal tumour on the bladder neck can be confirmed. Note the extensive local bladder wall thickening.

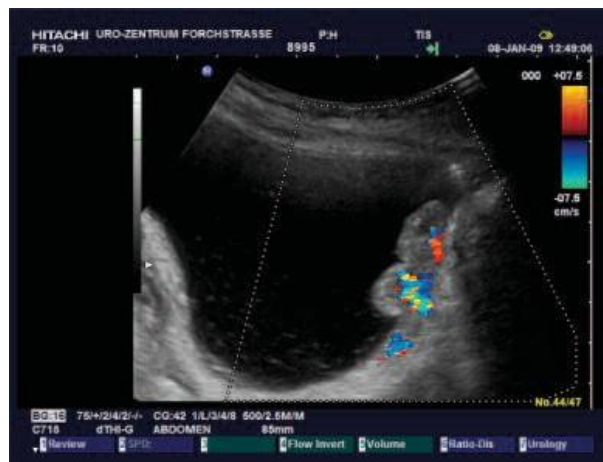


Figure 26 Contrast enhanced ultrasound (CEUS) has better sensitivity in the detection of low blood flow within a suspicious focal bladder lesion and can reliably diagnose transitional cell carcinomas. However, because cystoscopy and transurethral resection of the bladder tumour (TURBT) is mandatory, the use of CEUS in every suspicious bladder lesion is questionable because of cost.



Extravesical bladder infiltration (pT4 prostate cancer)

Ultrasound alone cannot discriminate between a primary bladder tumour (e.g. TCC) and tumours of other origins that infiltrate the bladder wall. A classic example is pT4 prostate cancer, which infiltrates the posterior bladder wall and often obstructs the distal ureter, resulting in hydronephrosis [(4, 5)].

Figure 27 Cystoscopic appearance of a pT4 Gleason score 4+4=8 prostate carcinoma, which has infiltrated the bladder floor. The macroscopic appearance of a solid transitional cell carcinoma G3 can look similar.



Pseudotumours

If ultrasound of the bladder is not performed adequately, prostate enlargement with median lobe hyperplasia may mimic a focal TCC, especially in cases with gross haematuria. A prominent interureteric crest, bladder folds or bladder trabeculation, especially in underfilled bladders, may also mimic TCC on ultrasound examination.

Figure 28 A 73 year old patient with painless macrohaematuria. Suprapubic ultrasound appearance mimics a large solitary spherical bladder tumour. However the appearance is actually caused by a large median lobe of prostatic hypertrophy.



Schistosomiasis

Schistosomiasis (also known as bilharziasis) is a parasitic infection caused by trematodes. It is endemic in Africa (especially along the River Nile in Egypt), Asia, Middle East and South America. The hosts are freshwater snails that release cercariae into the water. The infection is then transmitted to humans who drink or swim in contaminated water. Cercariae may migrate through intact skin to the subcutaneous vessels. The adult worm then migrates through the host's systemic circulation and releases eggs in different organs including the bladder, where they can be seen on cystoscopy. As a result of the high antigenic character of the eggs, granuloma formation and fibrosis are induced. *Schistosoma haematobium* is associated with an increased risk of bladder carcinoma [(6)]. Treatment for schistosomiasis consists of an oral dose of the anthelmintic, praziquantel .

Figure 29 View on cystoscopy of schistosomiasis lesions in the bladder mucosa of a patient from Africa.

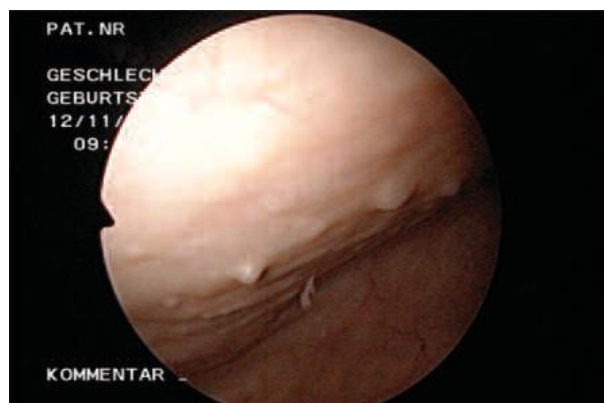


Figure 30 The same patient as Figure 29 presented with lower urinary tract symptoms. On bladder ultrasound with a high-frequency linear probe a calcified schistosomiasis egg within the bladder mucosa of the anterior wall is easily detectable (small yellow mark).



Endometriosis of the bladder

Endometriosis is caused by extrauterine spread of endometrial cells. These cells stay under the influence of female hormones during the menstrual cycle and can be the cause of pelvic pain during menstruation. If the bladder is affected by endometriosis, urinary urgency, frequency and painful voiding that worsens during menstruation are typically experienced [(7, 8)].

Figure 31 A young female with infertility, menstrual cycle dependent dysuria and urgency. Bladder ultrasound shows parauterine fluid accumulation with involvement of the bladder wall. A diagnosis of endometriosis of the bladder was proved on cystoscopy and transurethral bladder biopsy histology.



Diverticulum

Primary bladder diverticula are not common (incidence of 1.7%) and are a congenital malformation. A bladder diverticulum is the herniation of bladder mucosa through the bladder wall. Large diverticula can act as a paradoxical reservoir during bladder voiding. Post-void residual urine and urinary stasis can result in chronic urinary tract infection, stone formation and malignant urothelial transformation (i.e. TCC). Therefore diverticula, especially in those with a narrow neck, should be carefully examined during cystoscopy.

Figure 32 Solitary primary bladder diverticulum behind the enlarged prostate with middle lobe hyperplasia. Note the narrow neck of the diverticulum (4.4 mm).



Figure 33 Cystoscopy showing a bladder diverticulum. Note that there is only very slight trabeculation in contrast to the secondary acquired pseudodiverticula. This, together with diffuse bladder wall thickening and massive trabeculation are signs of chronic bladder outlet obstruction. The wall of a primary diverticulum lacks the normal muscularis layer, as a result the yellowish fatty tissue behind the bladder shines through the base of the diverticulum.

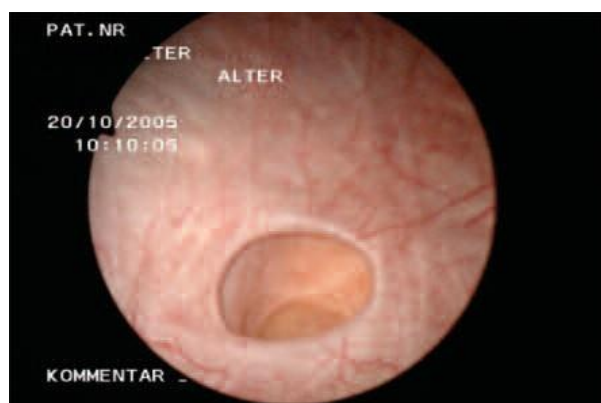


Figure 34 Bladder diverticulum. Note the location posterior to the prostate and the more hyperechoic content of the diverticulum compared with the bladder; this is as a result of urinary stasis with sludge formation and infection.



Endovesical intraluminal content (filling defects or intravesical masses)

In addition to the investigation of the bladder wall and shape, ultrasound examination of the bladder content can provide good diagnostic information about bladder pathology.

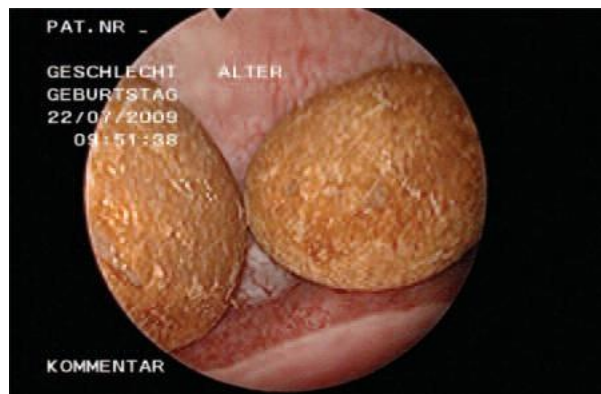
Bladder stones

Bladder calculi are the result of chronic lower urinary tract infections, usually due to incomplete voiding secondary to BOO or hypocontractile bladders [(9)]. Ultrasound can demonstrate stones with a typical stone shadow behind the hyperechoic stone [(10-13)]. Sometimes it is advisable to move the patient from a standard supine position to a lateral position in order to identify mobile bladder stones.

Figure 35 Bladder calculus in a male with bladder outlet obstruction. The twinkling artefact is not seen because of the even surface of calcium phosphate stones. The proof that this is a calculus is the shadow cast behind the stone. Only minimal twinkling artefacts can be demonstrated because of the relatively plain surface of stones (also seen Figure 34).



Figure 36 Cystoscopy in the same patient as Figure 35. Two large round stones with a plain surface can be seen inside the bladder.



Blood clot

As a complication following transurethral-bladder or transurethral-prostate surgery, post-operative bleeding may be present, especially if the patients are on antiplatelet therapy (e.g.

aspirin). Heavier bleeding may result in a blood clot, bladder tamponade and painful acute urinary retention, which is a urological emergency. In this condition, bladder ultrasound leads to a quick diagnosis and often correctly indicates the need for intervention.

Figure 37 Bladder ultrasound demonstrates a large coagulated haematoma in this patient post-operatively.



Indwelling catheter (double-J-catheter, bladder catheter)

Foreign bodies, bladder catheters and double-J ureteric catheters can be easily located on bladder sonography. The correct location of a double-J catheter (pigtail-catheter) inside the bladder and within the renal pelvis can be demonstrated with ultrasound, which is important in, for example, pregnancy hydronephrosis where radiography is contraindicated [(14-16)].

Figure 38 The sonographic appearance of a pigtail catheter is characterised by a typical hyperechoic double contour of the ureteric catheter. If there is some calcification on the catheter surface, 'stone shadowing' can be demonstrated.

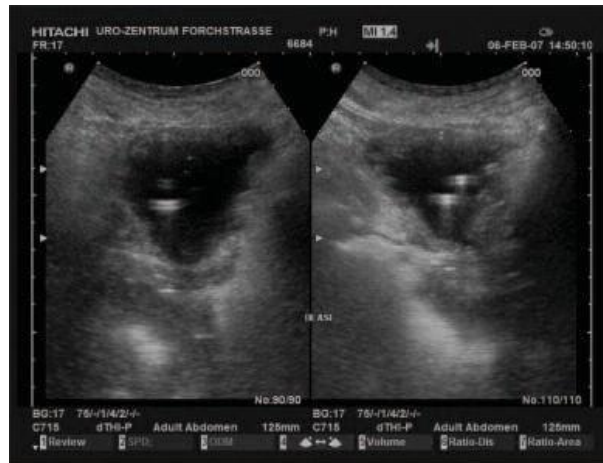


Figure 39 Cystoscopic view on the distal curl of a pigtail. Note the mucosal irritation owing to the foreign body.

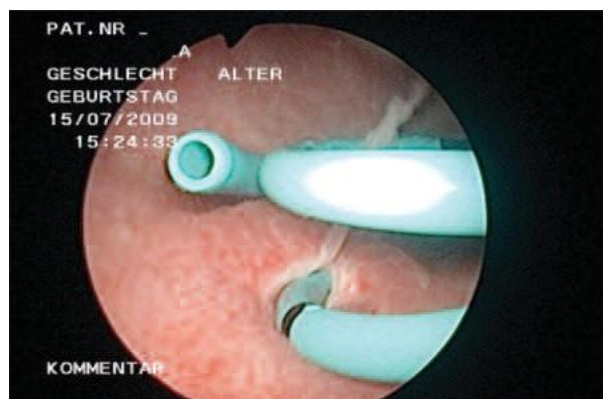


Figure 40 Cystoscopic view of the distal curl of a pigtail with early incrustation in a male patient with recurrent stone disease and hyperparathyroidism. The lumen is blocked by calcification.

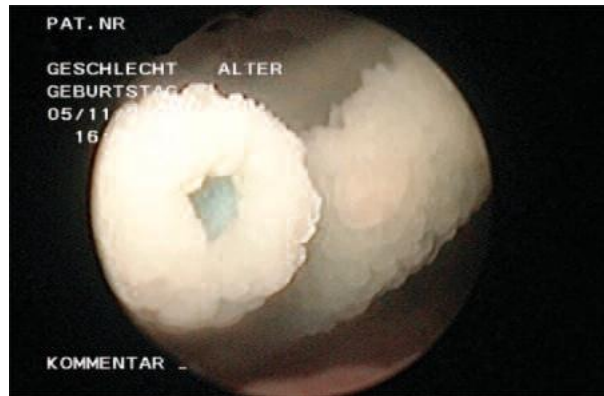
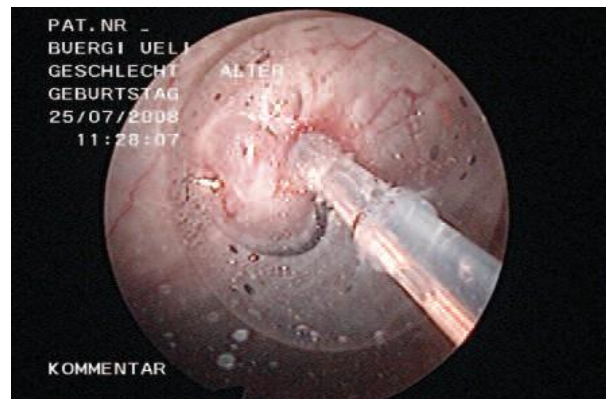


Figure 41 Transvaginal ultrasound of the bladder and urethra in a female patient with urethral diverticulum and a bladder catheter. Note the water blocked catheter balloon in the region of the bladder neck.



Figure 42 Cystoscopy showing correct location of a silicone 12-Fr suprapubic balloon catheter inside the bladder, which is blocked with glycerine solution.



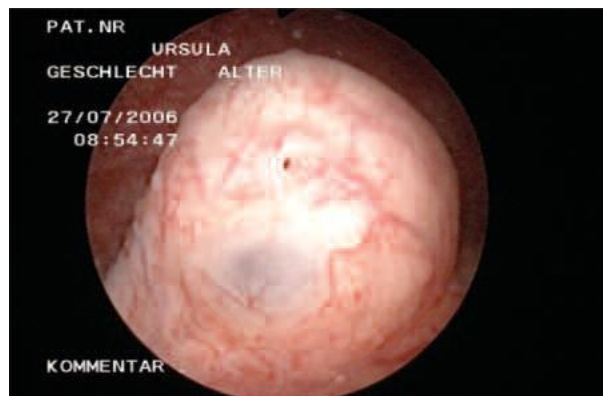
Ureterocoele

Ureterocoeles are ureteric anomalies appearing as cystic dilatations of the terminal ureter. They are four times more frequent in females. Only 10% are bilateral [(17-19)]. We can discriminate between orthotropic intravesical and ectopic ureterocoeles, which do not drain to the bladder. The later often cause incontinence or poor bladder emptying. Stasis of urine in the obstructed system often causes chronic infection and leads to secondary stone formation. Ureter anomalies are often concomitant with kidney malformations. The Meyer-Weigert rule describes the complete ureteric duplication. It states that the lower kidney pole ureter orifice inside the bladder is more cranial and lateral compared with the more caudomedial ostium of the upper pole kidney system. The routine use of ultrasound in pregnant mothers means that ureterocoeles are diagnosed prenatally. One method of treatment for obstructed ureterocoeles is transurethral incision.

Figure 43 Intravesical saccular outpouching of the distal ureter inside the bladder lumen with ureteric obstruction, hydroureter and stone formation.



Figure 44 Cystoscopy with ureterocele in the same female patient as Figure 40. Note the darker stone behind the translucent thin cystic ureterocele wall. Note the very restricted orifice of the ureter on the surface of this intravesical orthotopic single system ureterocele.



Air after cystoscopy or after catheterisation

Air below the bladder roof is often the result of transurethral manipulation, catheterisation or cystoscopy.

Figure 45 Post-void residual urine measurement after cystoscopy with hyperechoic air inside the bladder lumen.



Ureteric urine jet

Urine jet is the rhythmic expulsion of urine through the ureteric orifice (ostium) into the bladder. It can be visualised by real time colour Doppler ultrasound of the bladder. The diagnostic role is to identify the bladder trigone and assess the ureteric function particularly for the diagnosis of ureteric obstruction. The absence of unilateral urine jet may suggest unilateral obstruction owing to urolithiasis. Urine jets are not only seen on colour Doppler, but on B-mode grey scale ultrasound if there is a difference in the specific gravity of ureteric and bladder urine [(12, 13, 20)].

Figure 46 Ureteric urine jet is visible in this patient on B-mode ultrasound coming from the right ureteric orifice, and on colour Doppler coming out on the left ostium.

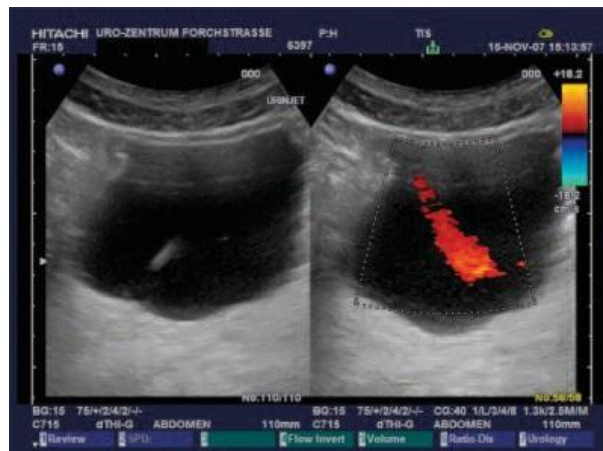
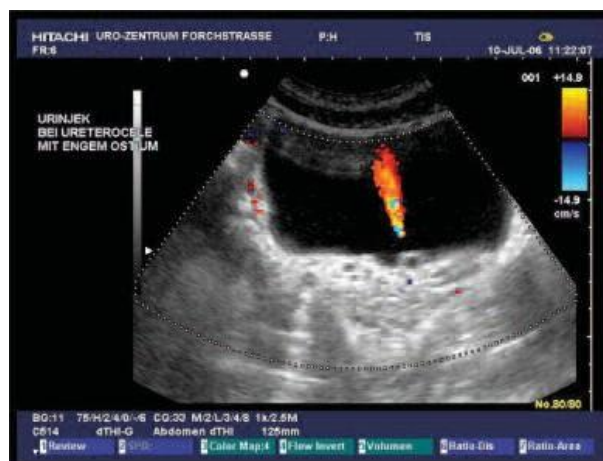


Figure 47 The quality of the jet is more rapid owing to flow obstruction by a ureterocoele with a restricted orifice. Note the more direct jet with high-velocity turbulence inside the jet (the change in flow direction is the blue colour inside the red jet directed towards the probe).



Extravesical abnormalities

In bladder ultrasound, it is important to assess the area surrounding the bladder. It is therefore crucial to know how full the bladder is. In an empty bladder there is no information

available on bladder pathology and there is greater potential for misinterpretation of extravesimal findings as bladder related pathology [(7, 8, 21-23)].

Pre-vesical ureter stone

Sonography of a filled bladder allows the pre-vesical ureter to be inspected. In cases where pre-vesical ureterolithiasis is suspected with the typical symptoms of pollakisuria and flank pain, the patient should be advised to attend bladder ultrasound with a full bladder [(10, 11, 24)].

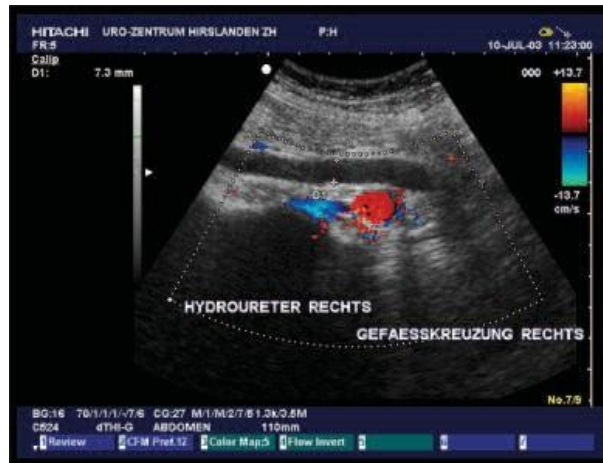
Figure 48 Pre-vesical ureter stone with a diameter of 5.2 mm. A stone shadow behind the calculus can be seen. There is no dilatation of the ureter.



Dilated hydroureter

In ureterolithiasis, stones often cause an obstruction at the level of the crossing of the ureter with the iliac vessel or pre-vesically. Using colour Doppler the iliac vessels can easily be identified and a dilated hydroureter can be seen on ultrasound, provided there is not too much gas in the colon [(15, 16, 25)].

Figure 49 Hydroureter over the iliac vessel crossing in a patient with an obstructing calculus within the distal ureter. Hydroureter at the right ureteric crossing with the iliac vessels.



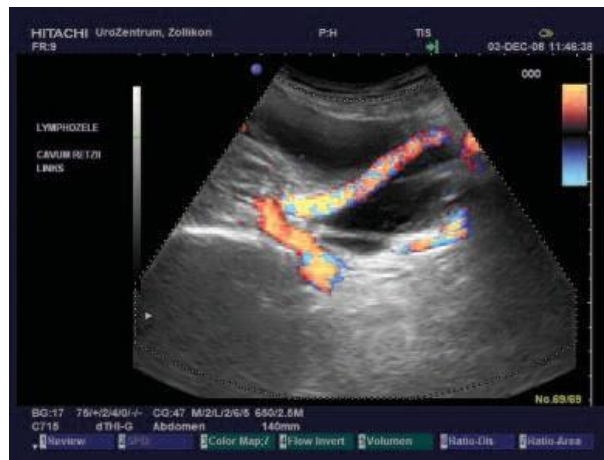
Lymphocoeles

Lymphocoeles can occur as a complication, for example after retropubic radical prostatectomy with lymphadenectomy. If the bladder is empty, a lymphocoele can mimic post-void residual urine.

Figure 50 Post-operative lymphocoele within Retzius' space, ventral to the bladder. With an empty bladder a big lymphocoele can often be misinterpreted as a filled or non-empty bladder.



Figure 51 Lymphocele around the iliac vessels in the region of the obturator triangle after pelvic lymphadenectomy in a prostate cancer case.



Ascites

As well as lymphocele, ascites can be misinterpreted as urine in an empty bladder in pelvic bladder ultrasound.

Figure 52 Ascites in a patient with metastatic colon cancer disease. Above the bladder there is fluid accumulation pushing the intestine cranially.



Extravesical tumours

When interpreting pathological findings inside the bladder with bladder ultrasound, it is crucial to know if the bladder is filled or empty. In the completely empty bladder, the bladder wall is often not detectable, which can lead to a misinterpretation of pathological findings around the bladder as bladder pathology [(21, 22)].

Figure 53 A female patient with a history of haematuria. Suprapubic ultrasound was performed as the first-line diagnostic test and it suggested papillary bladder cancer (i.e. transitional cell carcinoma (TCC)). Surprisingly no TCC was found inside the bladder on performing a cystoscopy.



Figure 54 The same patient as in the previous figure with bladder ultrasound after cystoscopy. Now the bladder is not empty and the pathological findings are seen to be related to the ovary. Post-operative histology confirmed a malignant cystadenocarcinoma of the right ovary.



Importance of bladder ultrasound in clinical practice

Ultrasound of the bladder is very important in routine patient evaluation in the urology clinic. It is the easiest way to evaluate bladder voiding in a non-invasive way by measurement of the post-void residual urine transabdominally. If bladder ultrasound is performed appropriately, it can provide detailed information of different diseases of the bladder in a non-invasive way and without the disadvantages associated with radiographs.

References

1. Babjuk M, Bohle A, Burger M, Capoun O, Cohen D, Comperat EM, Hernandez V, et al. EAU Guidelines on Non-Muscle-invasive Urothelial Carcinoma of the Bladder: Update 2016. *Eur Urol* 2017;71:447-461.
2. Sternberg CN, Skoneczna I, Kerst JM, Albers P, Fossa SD, Agerbaek M, Dumez H, et al. Immediate versus deferred chemotherapy after radical cystectomy in patients with pT3-pT4 or N+ M0 urothelial carcinoma of the bladder (EORTC 30994): an intergroup, open-label, randomised phase 3 trial. *Lancet Oncol* 2015;16:76-86.
3. Expert Panel on Urologic I, van der Pol CB, Sahni VA, Eberhardt SC, Oto A, Akin O, Alexander LF, et al. ACR Appropriateness Criteria((R)) Pretreatment Staging of Muscle-Invasive Bladder Cancer. *J Am Coll Radiol* 2018;15:S150-S159.

4. Barr RG, Cosgrove D, Brock M, Cantisani V, Correas JM, Postema AW, Salomon G, et al. WFUMB Guidelines and Recommendations on the Clinical Use of Ultrasound Elastography: Part 5. Prostate. *Ultrasound Med Biol* 2017;43:27-48.
5. Cosgrove D, Piscaglia F, Bamber J, Bojunga J, Correas JM, Gilja OH, Klauser AS, et al. EFSUMB guidelines and recommendations on the clinical use of ultrasound elastography. Part 2: Clinical applications. *Ultraschall Med* 2013;34:238-253.
6. Richter J, Botelho MC, Holtfreter MC, Akpata R, El Scheich T, Neumayr A, Brunetti E, et al. Ultrasound assessment of schistosomiasis. *Z Gastroenterol* 2016;54:653-660.
7. Dong Y, Braden B, Klinger C, Ripolles T, Dietrich CF. Ultrasound findings in extragenital endometriosis. *J Ultrason* 2018;18:247-254.
8. Saida T, Nakao S, Tanaka YO, Yano Y, Satoh T, Minami M. Urachal mucinous adenocarcinoma in the pelvic wall mimicking endometriosis. *Radiol Case Rep* 2018;13:955-959.
9. Takahashi S, Takei M, Nishizawa O, Yamaguchi O, Kato K, Gotoh M, Yoshimura Y, et al. Clinical Guideline for Female Lower Urinary Tract Symptoms. *Low Urin Tract Symptoms* 2016;8:5-29.
10. Sen V, Imamoglu C, Kucukturkmen I, Degirmenci T, Bozkurt IH, Yonguc T, Aydogdu O, et al. Can Doppler ultrasonography twinkling artifact be used as an alternative imaging modality to non-contrast-enhanced computed tomography in patients with ureteral stones? A prospective clinical study. *Urolithiasis* 2017;45:215-219.
11. Darge K, Heidemeier A. [Modern ultrasound technologies and their application in pediatric urinary tract imaging]. *Radiologe* 2005;45:1101-1111.
12. Tuma J, Jenssen C, Moller K, Cui XW, Kinkel H, Uebel S, Dietrich CF. [Ultrasound artifacts and their diagnostic significance in internal medicine and gastroenterology - Part 1: B-mode artifacts]. *Z Gastroenterol* 2016;54:433-450.
13. Jenssen C, Tuma J, Moller K, Cui XW, Kinkel H, Uebel S, Dietrich CF. [Ultrasound artifacts and their diagnostic significance in internal medicine and gastroenterology - part 2: color and spectral Doppler artifacts]. *Z Gastroenterol* 2016;54:569-578.
14. Cui XW, Ignee A, Maros T, Straub B, Wen JG, Dietrich CF. Feasibility and Usefulness of Intra-cavitary Contrast-Enhanced Ultrasound in Percutaneous Nephrostomy. *Ultrasound Med Biol* 2016.
15. Dietrich CF, Lorentzen T, Appelbaum L, Buscarini E, Cantisani V, Correas JM, Cui XW, et al. EFSUMB Guidelines on Interventional Ultrasound (INVUS), Part III - Abdominal Treatment Procedures (Long Version). *Ultraschall Med* 2016;37:E1-E32.
16. Dietrich CF, Lorentzen T, Appelbaum L, Buscarini E, Cantisani V, Correas JM, Cui XW, et al. EFSUMB Guidelines on Interventional Ultrasound (INVUS), Part III - Abdominal Treatment Procedures (Short Version). *Ultraschall Med* 2016;37:27-45.
17. Berte N, Vrillon I, Larmure O, Gomola V, Ayav C, Mazeaud C, Lemelle JL. Long-term renal outcome in infants with congenital lower urinary tract obstruction. *Prog Urol* 2018;28:596-602.
18. Johnson EK, Malhotra NR, Shannon R, Jacobson DL, Green J, Rigsby CK, Holl JL, et al. Urinary tract infection after voiding cystourethrogram. *J Pediatr Urol* 2017;13:384 e381-384 e387.
19. Chowdhary SK, Kandpal DK, Sibal A, Srivastava RN, Vasudev AS. Ureterocele in newborns, infants and children: Ten year prospective study with primary endoscopic deroofting and double J (DJ) stenting. *J Pediatr Surg* 2017;52:569-573.

20. Dietrich CF, Bartsch L, Turco V, Fröhlich E, Hocke M, Jenssen M, Kubale R, et al. Knöpfungologie in der B-Bild-Sonografie. *Gastroenterologie Up2date* 2018;14:347-367.
21. Atkinson NS, Bryant RV, Dong Y, Maaser C, Kucharzik T, Maconi G, Asthana AK, et al. WFUMB Position Paper. *Learning Gastrointestinal Ultrasound: Theory and Practice. Ultrasound Med Biol* 2016;42:2732-2742.
22. Atkinson NSS, Bryant RV, Dong Y, Maaser C, Kucharzik T, Maconi G, Asthana AK, et al. How to perform gastrointestinal ultrasound: Anatomy and normal findings. *World J Gastroenterol* 2017;23:6931-6941.
23. Dirks K, Calabrese E, Dietrich CF, Gilja OH, Hausken T, Higginson A, Hollerweger A, et al. EFSUMB Position Paper: Recommendations for Gastrointestinal Ultrasound (GIUS) in Acute Appendicitis and Diverticulitis. *Ultraschall Med* 2019.
24. Abdel-Gawad M, Kadasne R, Anjekar C, Elsobky E. Value of Color Doppler ultrasound, kub and urinalysis in diagnosis of renal colic due to ureteral stones. *Int Braz J Urol* 2014;40:513-519.
25. Mohaupt MG, Arampatzis S, Atkinson N, Yi D, Cui XW, Ignee A, Dietrich CF. Comments and extensions to EFSUMB guidelines on renal interventional ultrasound (INVUS). *Med Ultrason* 2016;18:351-361.